Junín Virus Promotes Autophagy To Facilitate the Virus Life Cycle

Julieta S. Roldán,[a] Nélida A. Candurra,[a] María I. Colombo,[b] ⃝ Laura R. Delgui[b,c]

aLaboratorio de Virología, Departamento de Química Biológica, IQUIBICEN, CONICET, Facultad de Ciencias Exactas y Naturales, Universidad de Buenos Aires (UBA), Buenos Aires, Argentina
bInstituto de Histología y Embriología de Mendoza (IHEM), CONICET, Facultad de Ciencias Médicas, Universidad Nacional de Cuyo, Mendoza, Argentina
cFacultad de Ciencias Exactas y Naturales, Universidad Nacional de Cuyo, Mendoza, Argentina

ABSTRACT Junín virus (JUNV), a member of the family *Arenaviridae*, is the etiological agent of Argentine hemorrhagic fever (AHF), a potentially deadly endemic-epidemic disease affecting the population of the most fertile farming land of Argentina. Autophagy is a degradative process with a crucial antiviral role; however, several viruses subvert the pathway to their benefit. We determined the role of autophagy in JUNV-infected cells by analyzing LC3, a cytoplasmic protein (LC3-I) that becomes vesicle membrane associated (LC3-II) upon induction of autophagy. Cells overexpressing enhanced green fluorescent protein (EGFP)-LC3 and infected with JUNV showed an increased number of LC3 punctate structures, similar to those obtained after starvation or bafilomycin A1 treatment, which leads to autophagosome induction or accumulation, respectively. We also monitored the conversion of LC3-I to LC3-II, observing LC3-II levels in JUNV-infected cells similar to those observed in starved cells. Additionally, we kinetically studied the number of LC3 dots after JUNV infection and found that the virus activated the pathway as early as 2 h postinfection (p.i.), whereas the UV-inactivated virus did not induce the pathway. Cells subjected to starvation or pretreated with rapamycin, a pharmacological autophagy inductor, enhanced virus yield. Also, we assayed the replication capacity of JUNV in Atg5 knockout or Beclin 1 knockdown cells (both critical components of the autophagic pathway) and found a significant decrease in JUNV replication. Taken together, our results constitute the first study indicating that JUNV infection induces an autophagic response, which is functionally required by the virus for efficient propagation.

IMPORTANCE Mammalian arenaviruses are zoonotic viruses that cause asymptomatic and persistent infections in their rodent hosts but may produce severe and lethal hemorrhagic fevers in humans. Currently, there are neither effective therapeutic options nor effective vaccines for viral hemorrhagic fevers caused by human-pathogenic arenaviruses, except the vaccine Candid no. 1 against Argentine hemorrhagic fever (AHF), licensed for human use in areas of endemicity in Argentina. Since arenaviruses remain a severe threat to global public health, more in-depth knowledge of their replication mechanisms would improve our ability to fight these viruses. Autophagy is a lysosomal degradative pathway involved in maintaining cellular homeostasis, representing powerful anti-infective machinery. We show, for the first time for a member of the family *Arenaviridae*, a proviral role of autophagy in JUNV infection, providing new knowledge in the field of host-virus interaction. Therefore, modulation of virus-induced autophagy could be used as a strategy to block arenavirus infections.

KEYWORDS *Arenaviridae*, Beclin 1, Junín virus, proviral role, replication, autophagy, innate immunity

Members of the family *Arenaviridae* are enveloped, negative-sense RNA viruses (1). The genus *Mammarenavirus*, comprising arenaviruses with mammalian hosts, has been divided into Old World (OW) and New World (NW) viral groups based on phylogenetic, serological, and geographical distribution differences (2). Mammarenaviruses cause chronic infections of rodents indigenous to Europe, Africa, America, and perhaps other continents. These asymptomatically infected animals move freely in their natural habitats and may invade human habitations. When humans come in contact with excreted viruses, disease may result. Arenavirus infections of humans are common and, in some cases, may cause severe disease. Indeed, several members of the group are responsible for severe acute infections termed hemorrhagic fevers (HF). Lymphocytic choriomeningitis virus (LCMV), the prototypic OW arenavirus with worldwide distribution, causes only mild, self-limiting illness in immunocompetent individuals, but Lassa virus (LASV) and Lujo virus (LUJV), OW arenaviruses distributed in Africa, can cause severe HF in humans (3, 4). On the other hand, the NW group is further subdivided into different clades: A, B, C, and the proposed new D (1). Among them, clade B contains many important human pathogens, such as Junín virus (JUNV) and Machupo, Sabia, Guaranito, and Chapare viruses. Among the above-listed pathogens, JUNV is the etiological agent of Argentine HF (AHF) (5). Currently, there are no effective therapeutic options, since no effective vaccines for viral HF caused by human-pathogenic arenaviruses exist, except the vaccine Candid no. 1 against JUNV in Argentina, used in areas of endemicity (6). To date, between hundreds and several thousand HF cases have been reported in the regions of endemicity, causing significant morbidity and high mortality; consequently, the viruses have been classified as category A pathogen agents by the U.S. National Institutes of Health. Therefore, since arenaviruses remain a severe threat to global public health, more comprehensive knowledge of the mechanisms of multiplication would improve our ability to fight the viruses.

Arenaviruses are enveloped, bisegmented, negative-strand RNA viruses (1). Each genomic RNA segment (L, 7.3 kb, and S, 3.5 kb) contains two open reading frames (ORFs) with opposite (ambisense) orientations divided by a noncoding intergenic region that serves as a transcription termination signal. The genomic-RNA segment L encodes the viral RNA-dependent RNA polymerase and the small zinc finger matrix protein Z, whereas segment S encodes the nucleoprotein (NP) and the viral glycoprotein (GP) precursor (GPC) (7). This precursor is proteolytically processed into a peripheral membrane glycoprotein (GP1), which is implicated in receptor binding; an integral glycoprotein (GP2); and the stable signal peptide (SSP), which may serve in envelope glycoprotein structure and trafficking (8).

The internalization of human-pathogenic arenaviruses into host cells has been extensively studied, especially regarding the receptor involved in this first step of the viral replication cycle. Several members of the OW complex and the NW clade C, containing the nonpathogenic Oliveros virus and Latino virus, use α-dystroglycan as a cellular receptor (9, 10). NW clade B arenaviruses employ transferrin receptor 1 (TfR1) of their natural hosts as the cellular receptor for viral entry, and it has been shown that all pathogenic members of the group use human TfR1 (hTFR1) to infect human cells (11). Additionally, some arenaviruses may use alternative receptors for entry. For example, for JUNV strain IV_{4454}, it has been demonstrated that the virus infection is enhanced by the presence of DC-SIGN (dendritic cell-specific intercellular adhesion molecule-3-grabbing nonintegrin) and L-SIGN (12). After internalization, exposure to the low-pH conditions of the late endosome is required to enhance membrane fusion by GPCs, which are reported to be unusually resistant to low pH (13). Whatever the internalization mechanism after entry into the host cell, viruses have evolved a plethora of mechanisms to gain control of critical cellular signaling pathways that affect broad aspects of cellular macromolecular synthesis, metabolism, growth, and survival for their benefit.

Autophagy is an essential lysosomal degradation pathway that controls cellular homeostasis by eliminating protein aggregates and damaged organelles from the

cytoplasm. The pathway, initially identified as a cellular starvation-induced process, constitutes an evolutionarily conserved response in eukaryotes enabling the degradation of proteins, carbohydrates, and lipids, which allows the cell to adapt its metabolism and meet its energy needs (14). Autophagy may be deregulated in several disorders, including metabolic diseases, neurodegenerative disorders, infectious diseases, and cancer. Autophagy is also an essential contributor to both innate and adaptive immunity against intracellular pathogens (15). The pathway begins with the formation of isolation membranes in the cytoplasm known as phagophores, which elongate and surround the cytoplasmic cargo to form double-membrane vesicles called autophagosomes. During this stage, the microtubule-associated protein 1 light chain 3 (LC3-I) becomes covalently linked to phosphatidylethanolamine (PE) and is incorporated into autophagosome membranes. This lipidation process converts cytosolic LC3-I into the active, autophagosome membrane-bound form, LC3-II. Autophagosomes move toward the microtubule-organizing center, where there is a perinuclear concentration of lysosomes. Ultimately the autophagosomes fuse with the acidic lysosomes to form the autolysosome, where degradation and eventual recycling of the resulting macromolecules occur (16).

In the last few years, there have been multiple studies on the role of autophagy in virus replication cycles (17). An example of a specific antiviral action is the targeting of the pathogen to autophagosomes, a process called xenophagy or virophagy, whereby activation of autophagy leads to the sequestering of cytoplasmic subviral components in autophagosomes for lysosomal degradation. Therefore, many highly successful pathogens have evolved mechanisms to evade the deleterious autophagic effects and, in some cases, to subvert the pathway to promote their replication. For example, several single-stranded RNA viruses, such as poliovirus, coronavirus, dengue virus, and hepatitis C virus, seem to induce the accumulation of autophagic vacuoles and use these membrane vesicles to benefit their replication (18–20). In contrast, other viruses, such as herpes simplex virus 1 (HSV-1), human cytomegalovirus, and Kaposi's sarcoma herpesvirus, have evolved mechanisms to suppress autophagy and, in the case of HSV-1, favor its survival (21–23). However, to date, the role of autophagy in arenavirus infection remains unknown. Here, we intended to define the role of autophagy in JUNV replication to provide a basis for further studies of the life cycle of arenaviruses, analyzing the biological significance of autophagy in JUNV replication *in vitro*. We found that JUNV induces autophagy at early times after infection. In contrast, UV-inactivated virus did not trigger the autophagic response. We assayed the replication capacity of JUNV in Atg5 knockout or Beclin 1 knockdown cells (both critical components of the autophagic pathway) and found a significant decrease in JUNV replication. Taken together, our results constitute the first study indicating that JUNV replication induces an autophagic response that is in turn functionally required by the infecting virus for efficient propagation.

RESULTS

JUNV infection activates the autophagy pathway. Viruses have evolved diverse mechanisms to exploit cellular processes in order to coexist with their hosts and to evade host defenses. One central cell pathway is an ancient degradative process, designated autophagy. Even though cumulative evidence indicates that many viral agents interact with the autophagic pathway (reviewed in reference 24), there is no evidence indicating whether JUNV infection modulates autophagy. Therefore, we decided to explore JUNV-induced autophagy modulation by employing human lung epithelial A549 cells as the cellular model. First, we analyzed autophagy pathway modulation in these cells by employing well-known autophagy modulators and JUNV infection by performing immunoblotting with an antibody against LC3. During the course of autophagy, the cytosolic LC3 form (LC3-I) undergoes a process modifying it into a phosphatidylethanolamine-conjugated form (LC3-II), which can associate with the autophagosomal membranes (25). LC3-I and LC3-II are easily separated by SDS-PAGE because of the difference in their electrophoretic mobilities, and the level of
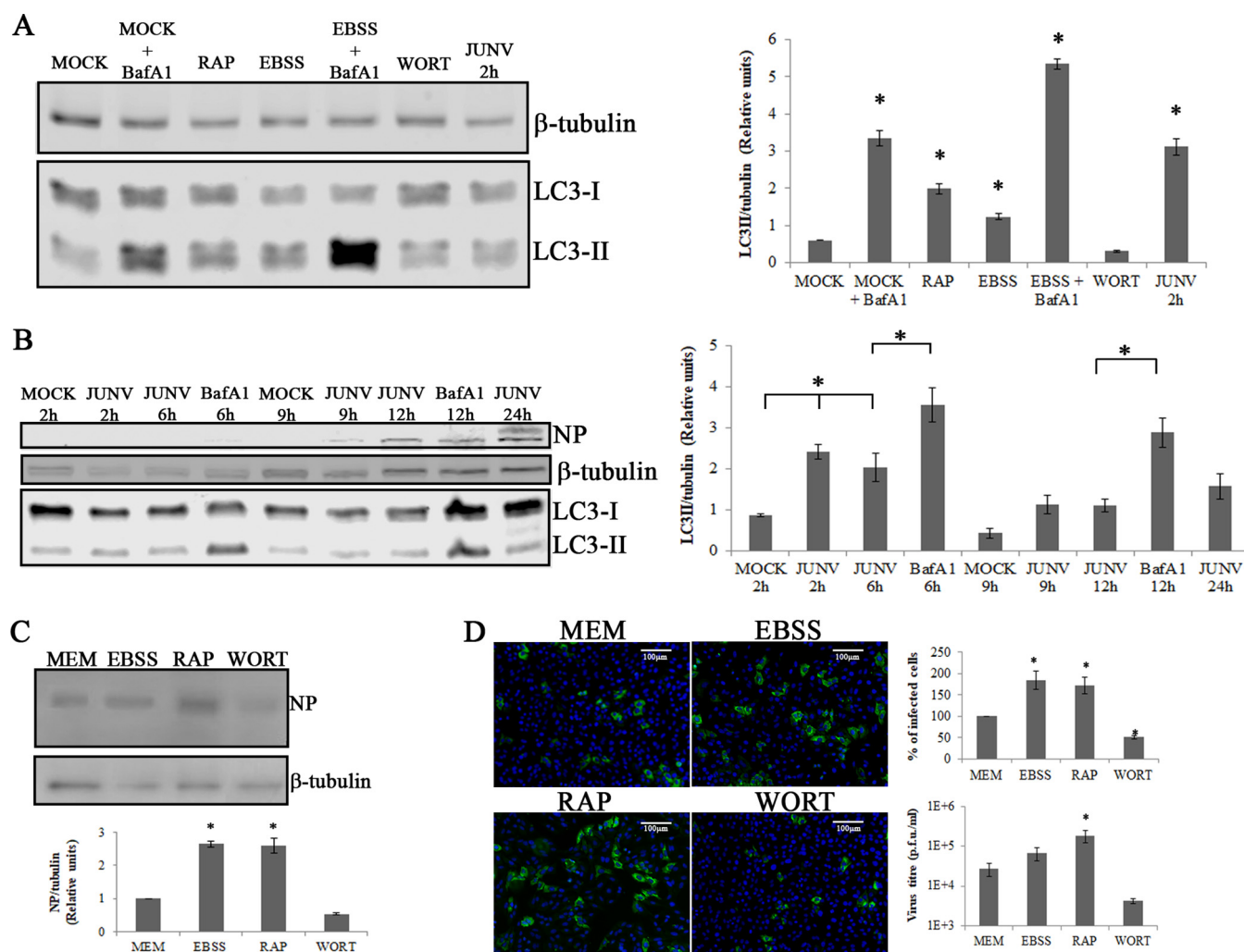
FIG 1 JUNV infection induces the autophagy pathway. (A) A549 cells were treated with MEM (MOCK), MEM plus 100 nM BafA1, 100 nM RAP, EBSS, EBSS plus 100 nM BafA1, or 100 nM WORT or infected with JUNV at an MOI of 1. After 2 h of treatment, the cells were processed for Western blot analysis. *, $P < 0.05$. (B) A549 cells were mock treated or infected with JUNV at an MOI of 1. At 5 and 11 h p.i., BafA1 was added for 1 h before processing. A rabbit polyclonal anti-LC3 antibody, monoclonal antibodies against the JUNV NP, and a monoclonal antibody against β-tubulin were used, followed by the corresponding peroxidase-conjugated secondary antibodies. The quantifications of the Western blot were conducted as described in Materials and Methods. *, $P < 0.05$. (C and D) A549 cells were treated with EBSS, RAPA, WORT, or MEM for 2 h and then infected with JUNV at an MOI of 1; 24 h p.i., the cells were processed for Western blot or immunofluorescence analysis. (C) After 24 h, cells were processed for Western blot analysis using monoclonal antibodies against the JUNV NP and a monoclonal antibody against β-tubulin, followed by the corresponding peroxidase-conjugated secondary antibodies. The quantifications of the Western blot analysis were conducted as described in Materials and Methods. *, $P < 0.05$. (D) At 24 h p.i., supernatants were harvested, and titers were determined by a PFU assay. Also, in order to determine the percentage of infected cells, samples were fixed and processed for immunofluorescence assay to detect viral NP, as described in Materials and Methods, and the nuclei were stained with Hoechst stain (magnification, $\times$100; *, $P < 0.05$). The data represent means and SE. In all cases, a representative experiment from three independent experiments is shown.

LC3-II correlates with the number of autophagosomes in the cell. Monolayers of the human cell line A549 were mock treated or treated for 2 h with bafilomycin A1 (BafA1), which blocks the autophagy flux with a concomitant increase in the levels of LC3-II; rapamycin (RAP), a widely used compound that induces autophagy (26); Earle's balanced salt solution (EBSS) (GIBCO), for starvation induction of the pathway; EBSS plus BafA1; and wortmannin (WORT), which exercises inhibitory effects on class III phosphatidylinositol-3 kinase (PI3K) activity, which is required for autophagy initiation (27); or JUNV at a multiplicity of infection (MOI) of 1. Because the ratio between LC3-II and housekeeping gene expression is considered an accurate indicator of autophagic activity, we assessed the densitometric ratios of LC3-II to β-tubulin. As shown in Fig. 1A, a small fraction of processed LC3-II was detected under normal conditions, whereas processed LC3-II was significantly increased in cells after exposure to BafA1, RAP, EBSS,

or EBSS plus BafA1. Also, as expected, WORT treatment caused inhibition of the pathway with less accumulation of the LC3-II form than with control-treated cells. Furthermore, in JUNV-infected cells, we observed a significant increase in the accumulation of the LC3-II form after 2 h of infection, as shown in Fig. 1A. Therefore, we decided to further explore this observation by performing a time course infection (2, 6, 9, 12, and 24 h of infection) followed by Western blot analysis of LC3-II. In order to do this, monolayers of A549 cells were infected with JUNV at an MOI of 1, and monoclonal antibodies against JUNV nucleoprotein, which specifically recognize JUNV NP, were employed to estimate the infection progress. As expected, JUNV NP was detected from 9 h postinfection (p.i.) and increased during the 24 h of infection, which is in concordance with the ordinary course of infection. The results shown in Fig. 1B demonstrate a significant increase in LC3-II levels in JUNV-infected cells relative to mock-treated cells (Fig. 1B, MOCK) at 2 and 6 h p.i., as indicated by the LC3-II/β-tubulin ratio. To determine whether LC3-II accumulation was due to autophagy induction or to a block in the maturation of autophagosomes into autolysosomes (28), we employed BafA1, which can distinguish between the two possibilities (29). Therefore, we treated infected cells for 1 h with the compound at two time points after infection, 5 and 11 h p.i. As shown in Fig. 1B, we observed a significant increase in LC3-II levels after BafA1 treatment of infected cells compared to 6 or 12 h p.i. without BafA1 treatment, suggesting that the virus does not alter the autophagic flux but likely induces the autophagy pathway. Similar results were obtained when we inhibited lysosomal proteolysis, employing pepstatin A as an alternative approach (data not shown).

Next, in order to study if autophagy modulation was able to impact viral infection, we pretreated cells with well-established autophagy inducers and inhibitors, followed by infection of A549 cells with JUNV. For this purpose, monolayers of the human cell line A549 were treated for 2 h with EBSS, RAP, or WORT or left with minimum essential medium (MEM)-10% fetal calf serum (FCS) (control). Then, the cells were infected with JUNV at an MOI of 1, fixed at 24 h p.i., and subsequently subjected to Western blot analysis to detect the viral NP under the different conditions tested. As shown in Fig. 1C, the levels of viral NP were significantly increased in EBSS- or RAP-pretreated monolayers, where the autophagy pathway was previously induced. In order to confirm these data, a different set of monolayers, similarly treated, were immunostained for detection of the viral NP to determine the extent of infection by epifluorescence microscopy, as well as by titrating the virus in the supernatant. As shown in Fig. 1D, the percentage of infected cells was significantly higher in the monolayers pretreated with EBSS or RAP. Accordingly, viral titer was significantly increased after autophagy induction by RAP treatment. The WORT treatment exerted a partial effect on infection, but we did not observe statistical significance, probably due to a weak effect of the drug on basal autophagy. Altogether, these results suggest that JUNV infection induces the autophagy pathway early p.i., with a proviral role of the pathway, demonstrated by the increased percentage of infected cells after pretreatment of the cells with autophagy inducers.

Autophagic flux is not affected by JUNV infection. In order to corroborate that the increased accumulation of autophagosomes in infected cells corresponded to an induction of the biogenesis of autophagosomes rather than to a block of their fusion with lysosomes, we performed an additional assay employing the tandem fusion of LC3 with the red, acid-insensitive mCherry (red fluorescent protein) and the acid-sensitive green fluorescent protein (GFP) to quantify the autophagic flux (30). Thus, mCherry-GFP-LC3-transfected cells were infected with JUNV at an MOI of 1 and fixed at 2, 6, 9, 12, and 24 h p.i., and the numbers of autophagosomes (GFP$^+$, mCherry$^+$, or yellow puncta) and autophagolysosomes (GFP$^-$, mCherry$^+$, or red puncta) were determined by using confocal microscopy images. We used mock treatment, mock treatment plus BafA1, EBSS-starved cells, and EBSS plus BafA1 as internal controls and GP antibodies to identify infected cells in our kinetics of JUNV infection. The autophagolysosome/autophagosome ratio was determined for each condition and employed to analyze the

effect of JUNV infection on the pathway. We observed a significant increase in the total number of autophagic structures with a ratio similar to that under EBSS conditions after 2, 6, and 24 h of infection, reinforcing our previous results pointing to induction of the pathway by the presence of the virus (Fig. 2).
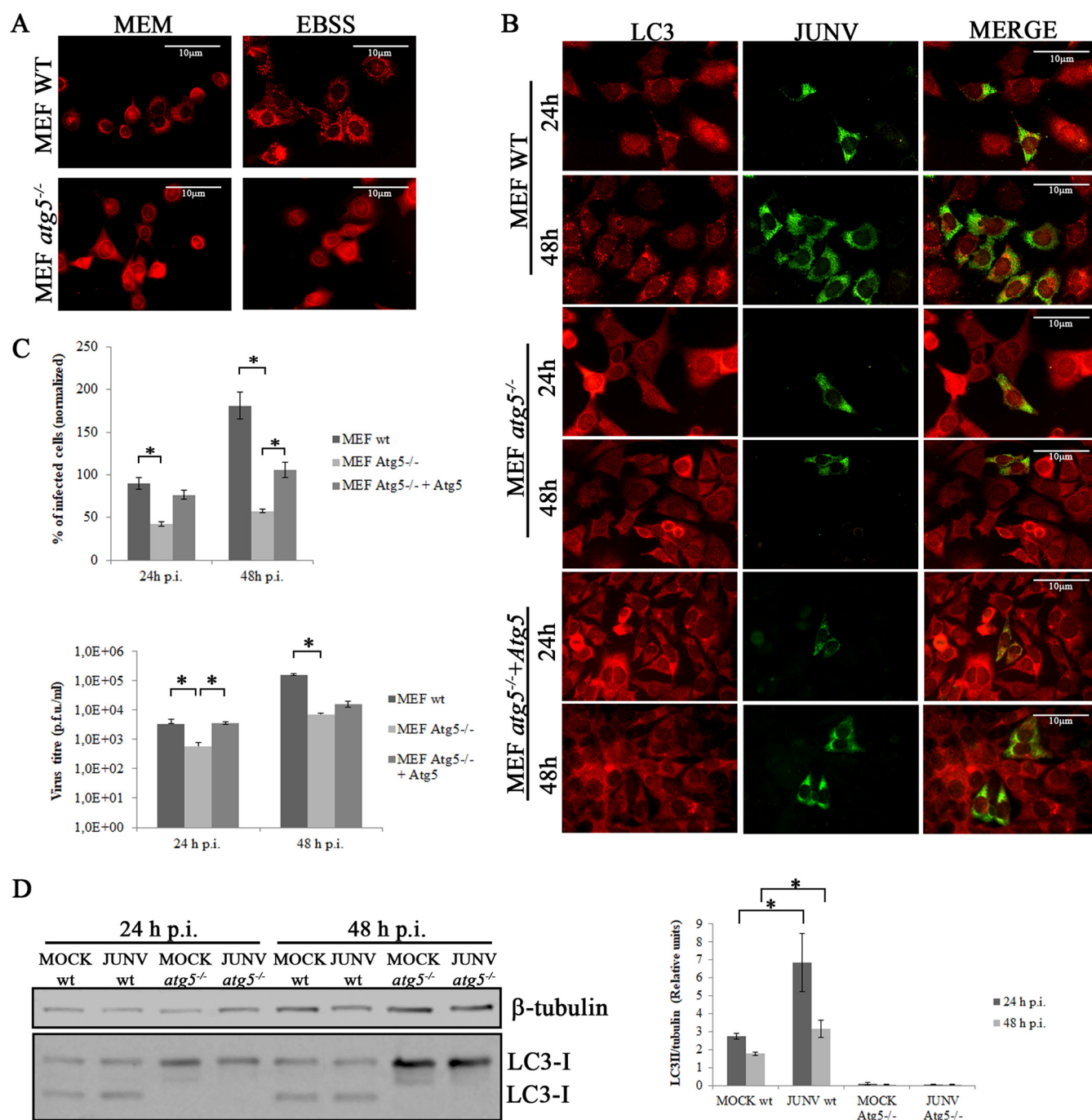
JUNV requires the autophagy protein Atg5. To further validate our observations, we analyzed JUNV replication in wild-type (WT) and *atg5*$^{-/-}$ mouse embryonic fibroblasts (MEFs). Atg5 is an essential protein for autophagosome formation (31). Indeed, these cells have been widely used to study the relationship between viral infections and autophagy (32–34). Before employing the *atg5*$^{-/-}$ cells in our viral assays, we validated their autophagy deficiency. Therefore, we monitored basal autophagosomal levels in rich medium (MEM), as well as under induced autophagy conditions (EBSS). As expected, WT MEFs showed a punctate distribution of endogenous LC3 protein after EBSS treatment (Fig. 3A, top), whereas in *atg5*$^{-/-}$ MEFs, the LC3-specific signal remained cytoplasmic (Fig. 3A, bottom). Then, to examine the role of ATG5 in JUNV infection, we infected WT, *atg5*$^{-/-}$, and Atg5-overexpressing *atg5*$^{-/-}$ MEFs at an MOI of 1. At 24 h and 48 h p.i., the cells were fixed, immunostained for endogenous LC3 and the viral protein NP, and analyzed by epifluorescence microscopy as shown in Fig. 3B. Notably, at both 24 and 48 h p.i., infected WT MEFs showed a clear punctate pattern for endogenous LC3, demonstrating autophagy induction in the cells. Interestingly, as shown in Fig. 3C, the percentage of infected cells (determined by the expression of NP) was significantly lower in *atg5*$^{-/-}$ MEFs than in WT MEFs at both times p.i. analyzed. Additionally, at 48 h p.i., we observed significant recovery of the percentage of infected cells when we complemented the *atg5*$^{-/-}$ MEFs by transfecting them with a plasmid construct encoding Atg5. Then, to quantitatively confirm the effect of autophagy deficiency on the ability of the virus to complete its replication cycle, we performed viral titration by employing the supernatants from 24 and 48 h p.i. of infected WT, *atg5*$^{-/-}$, and Atg5-overexpressing *atg5*$^{-/-}$ MEFs. We observed that the JUNV yield was significantly decreased in *atg5*$^{-/-}$ MEFs, with significant recovery at 24 h p.i. after complementation compared to the WT cells, reinforcing the notion that Atg5 is required for the JUNV infection cycle (Fig. 3C).

Finally, we conducted Western blot analysis of WT and *atg5*$^{-/-}$ infected MEFs, confirming two aspects of our study: (i) the accumulation of LC3-II in infected WT MEFs (Fig. 3D, bottom) and (ii) the absence of LC3-II formation in *atg5*$^{-/-}$ MEFs after JUNV infection, which suggests that autophagy induction by JUNV infection is Atg5 dependent. Interestingly, *atg5*$^{-/-}$ MEFs showed higher basal levels of LC3-I than WT MEFs, consistent with the fact that LC3-I cannot be processed into LC3-II in these cells and suggesting that JUNV autophagy induction occurs upstream of the Atg5-dependent step (Fig. 3D, bottom).

JUNV requires the autophagy protein Beclin 1. The autophagy-related proteins Atg5 and Atg7, as well as Beclin 1 and the class III PtdIns3K, all play important roles in conventional autophagy (35). Canonical (Beclin 1-dependent) autophagy activation is usually initiated by the formation of the Beclin 1-PtdIns3K complex, which is comprised of Beclin 1, PtdIns3K, PIK3R4/VPS15, and UV irradiation resistance-associated gene (UVRAG) or Atg14 (39). During activation of Beclin 1-dependent autophagy by stimulants such as serum starvation, phosphatidylinositol-3-phosphate (PtdIns3P) is generated by the enzymatic activity of the Beclin 1-PtdIns3K complex and recruited to the membrane for autophagosome formation (36). However, increasing evidence suggests that specific noncanonical autophagy (Beclin 1 independent) (37) can be induced independently of Beclin 1 or PtdIns3K in several cell types by specific stimulants or infection by pathogens (38–43). Thus, to test whether JUNV-induced autophagy relies on the canonical or noncanonical pathway, we decided to perform a second genetic study using small interfering RNAs (siRNAs) against Beclin 1. We used a plasmid carrying a small interfering RNA against Beclin 1 (pSuper Beclin 1-KD, referred to as Beclin 1-KD), which causes knockdown of transfected cells after 48 h. A549 cells were first transfected, and at 24 h posttransfection, the cells were infected with JUNV at an MOI of 1,
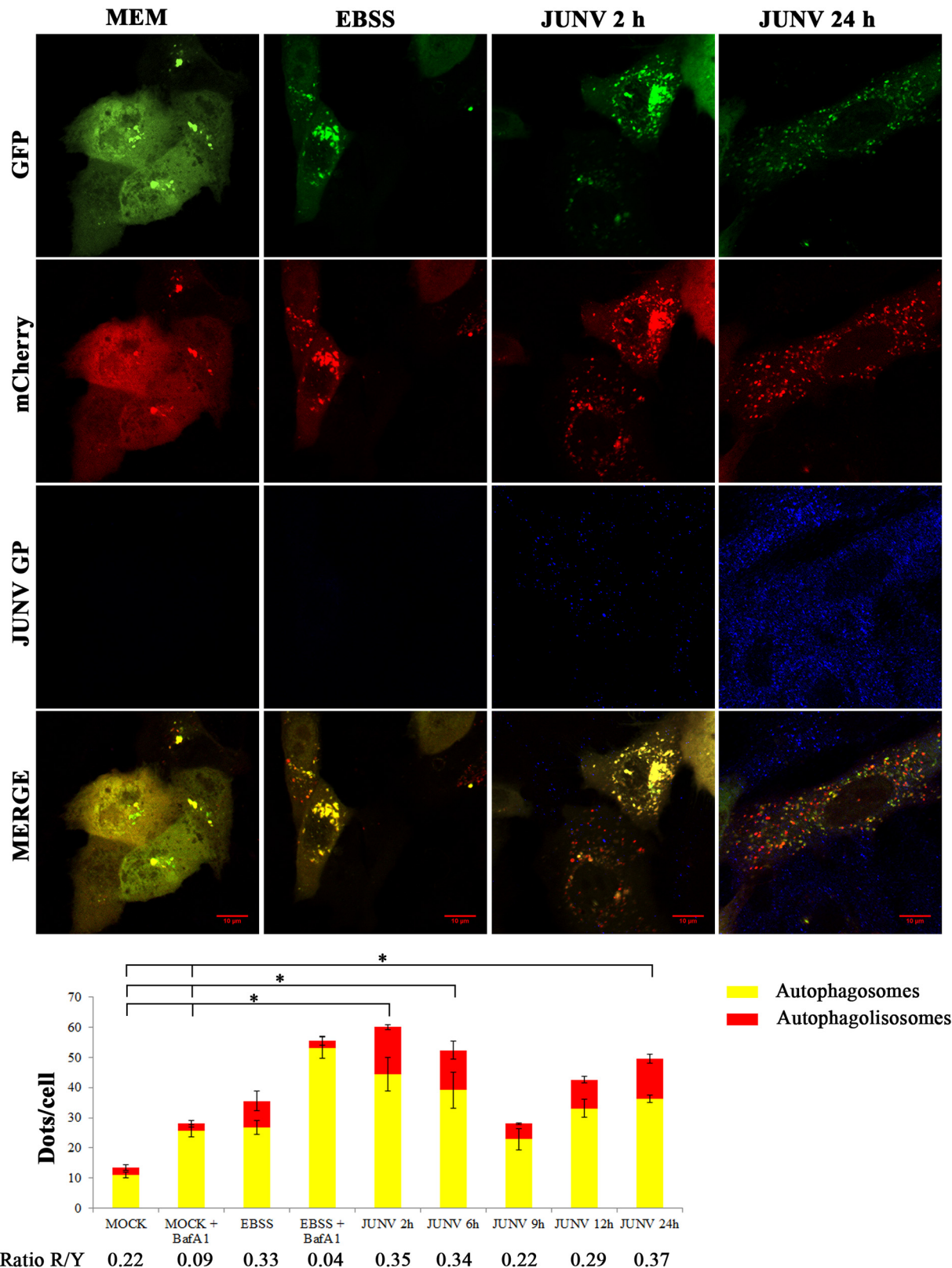
FIG 2 JUNV infection promotes autophagic induction. A549 cells were transfected with a plasmid encoding the mCherry-GFP-LC3 tandem construct or with the empty construct. Twenty-four hours posttransfection, the cells were treated with MEM (MOCK) or MEM plus 100 nM BafA1, and the numbers of red and yellow punctate structures were determined. Two-tailed ANOVA with Tukey's test contrast was used to determine statistical significance, considering the total number of dots (red plus yellow) under each condition (*, $P < 0.05$). The ratio of red dots to yellow dots (Ratio R/Y) was also determined as a measure of the autophagy flux. Representative images were taken using a confocal microscope (Olympus FV 1000). The data represent means and SE. In all cases, a representative experiment from three independent experiments is shown.

FIG 3 Efficient JUNV replication requires the autophagy protein Atg5. (A) WT and *atg5⁻/⁻* MEFs were treated with MEM or EBSS for 2 h and then fixed and processed for immunofluorescence assay using an LC3 antibody (magnification, ×400). (B to D) Both types of MEF and the Atg5-complemented *atg5⁻/⁻* MEFs were infected with JUNV at an MOI of 1. At 24 and 48 h p.i., the supernatants were collected, and the cells were fixed and processed for immunofluorescence using LC3 (red) and NP (green) antibodies. The numbers of infected and total cells were determined and then related to the control treatment (panel C) (*, $P < 0.05$). (C) Titers of the supernatants harvested 24 and 48 h p.i. were determined by PFU assay (*, $P < 0.05$). (D) Cells were processed for Western blotting 24 and 48 h p.i. LC3 and β-tubulin antibodies were used. The protein band quantification was conducted as described in Materials and Methods. The data represent means and SE. In all cases, a representative experiment from three independent experiments is shown.

and infection was allowed to proceed for a total of 24 h. The expression levels of Beclin 1 and the extent of infection were analyzed by Western blotting, as shown in Fig. 4A. We observed a significant decrease in both Beclin 1 expression and viral NP accumulation in the Beclin 1-KD-transfected cells compared to those transfected with the empty vector, pSuper, corroborating the knockdown of protein expression and the
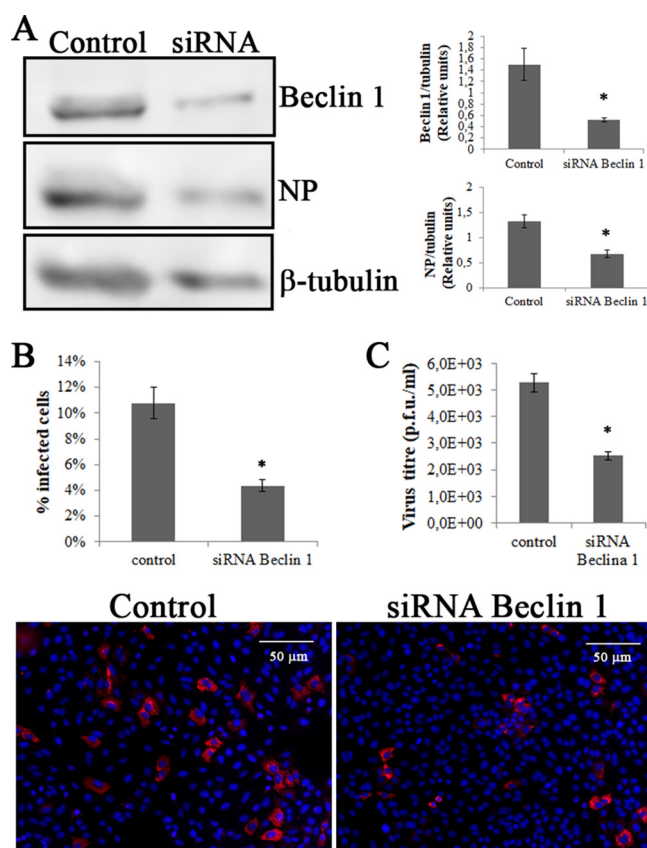
FIG 4 JUNV requires the autophagic protein Beclin 1. A549 cells were transfected with a plasmid encoding a pSuper Beclin 1 (siRNA) construct or the empty construct (control). Twenty-four hours posttransfection, the cells were infected with JUNV at an MOI of 1 or mock treated. Twenty-four hours p.i., the cells were fixed and processed for Western blotting (A) or immunofluorescence analysis (B). (A) Monoclonal antibodies against Beclin 1, JUNV NP, and β-tubulin were used, followed by the corresponding peroxidase-conjugated secondary antibodies. The quantifications of the Western blot analysis were conducted as described in Materials and Methods (*, $P < 0.05$). (B) A monoclonal antibody against the JUNV NP was used as described in Materials and Methods to detect infected cells. Nuclei were stained with Hoechst stain in order to determine the percentage of infected cells (*, $P < 0.05$). (C) Supernatants were harvested, and titers were determined by a PFU assay (*, $P < 0.05$). The data represent means and SE. In all cases, a representative experiment from three independent experiments is shown.

concomitant hampering of the viral life cycle (Fig. 4A). Subsequently, to quantitatively assay the effect of autophagy deficiency on the ability of the virus to complete its replication cycle, we infected knocked down and control A549 cells with JUNV at an MOI of 1, and at 24 h p.i., the cells were fixed, immunostained for the viral NP, and analyzed by epifluorescence microscopy as shown in Fig. 4B. As shown, the percentage of infected cells (determined by the expression of NP) was significantly lower in the Beclin 1-KD-transfected monolayers than in those transfected with the empty vector. At the same time, the supernatants were harvested and employed for viral titration under both conditions. As expected, we observed that the JUNV yield was significantly decreased in the cells with a diminished level of Beclin 1 compared to those with regular protein expression (Fig. 4C). Altogether, our observations powerfully depict a scenario where the presence of the virus inside the host cells triggers the induction of the canonical (Beclin 1-dependent) pathway by stimulation of autophagosome biogenesis without significantly affecting the autophagic flux. More importantly, autophagy seems to be crucial for viral infection establishment.

JUNV infection induces the autophagy pathway in a viral protein expression-dependent fashion. Next, and already focusing on the elucidation of the autophagy induction mechanism, we decided to analyze whether the modulation of the autophagic pathway was dependent on viral replication. To address this issue, A549 cells

were transfected with pEGFP-LC3, and 24 h posttransfection, the cells were treated with MEM, EBSS, BafA1, RAP, or WORT or infected with JUNV at an MOI of 1 for 2 or 6 h. To assess whether the induction of autophagy observed in JUNV-infected cells requires the expression of viral proteins, we used UV-inactivated JUNV, which can interact with cellular receptors and enter cells but does not exhibit any viral gene expression. Then, the cells were fixed and processed for direct confocal microscopy analysis of enhanced green fluorescent protein (EGFP)-LC3. In infected cells, fixation and immunodetection of the viral GP were performed (shown in Fig. 5A, top). It is essential to mention that at 6 h p.i. with UV-inactivated JUNV, the vast majority of cells showed weak or absent specific GP signal, probably due to lysosomal degradation of the inactivated particles. As shown in Fig. 5A (bottom), after the treatment of A549 cells with EBSS, BafA1, or RAP, we observed an increase in the number of punctate structures per cell, while WORT treatment caused a decrease in the number of LC3 puncta compared with the MEM-treated control. In the infected coverslips, the number of puncta of EGFP-LC3 per cell was measured only in infected cells, which exhibited GP (red) staining. Interestingly, at both time points assayed, we observed significant accumulation of EGFP-LC3 punctate structures in JUNV-infected cells, while no difference was observed when the cells were infected with UV-inactivated JUNV (Fig. 5A). To confirm this result, we conducted a Western blot analysis of infected A549 cells and used an anti-EGFP antibody in order to analyze the EGFP–LC3-II/β-tubulin ratio. EGFP–LC3-II conversion in A549 cells infected with JUNV or UV-inactivated JUNV was analyzed, and significant increases in the EGFP–LC3-II/β-tubulin ratio at 2 and 6 h p.i. were observed only when the virus was infective (Fig. 5B). These remarkable results indicate that the early induction of the autophagy pathway by JUNV is dependent upon the viral replication ability within the host cells.

DISCUSSION

The autophagy pathway is a crucial component of host defense against viral infection, leading to pathogen degradation, innate immune response, and also specific features of adaptive immunity. However, to survive and propagate within the host, viruses have evolved a plethora of strategies to evade the autophagic fight and to manipulate the autophagy machinery for their benefit. To date, the relationship between JUNV (or, indeed, any arenavirus) infection and autophagy has not been analyzed. Therefore, we intended to define the role of autophagy in JUNV replication to provide the basis for further studies of the arenavirus life cycle, analyzing the biological significance of autophagy in JUNV replication *in vitro*. Our study clearly showed that JUNV infection triggers an increase in the conversion of LC3-I to LC3-II and accumulation of autophagic structures in a Beclin 1-dependent fashion in permissive human A549 cells from 2 h p.i., indicating the early activation of the canonical autophagic pathway after viral infection. To dissect if this effect was due to autophagy induction or flux blocking, we employed BafA1, a proton pump V-ATPase inhibitor that hampers autophagy progression; pepstatin A, a lysosomal protease inhibitor (data not shown); and the tandem fusion protein mCherry-GFP-LC3, all of them well-described tools to analyze autophagy flux modulation (30). As mentioned above, arenavirus entry is initiated by binding to an appropriate cell surface receptor protein, hTfR1 in the case of the pathogenic NW viruses (11, 44). After binding to hTfR1, the virion is endocytosed, and the viral and endosomal membranes fuse, a process activated by the acidification of the maturing endosome (45, 46). This fusion event promotes viral uncoating, allowing the viral core to initiate its replication in the cytoplasm. Thus, we assayed BafA1 treatments in JUNV infections at 5 and 11 h p.i. in order to dissect autophagy induction from autophagy flux blocking after JUNV infection without interfering with viral entry and progression of the infection. The marked increase in LC3-II accumulation after BafA1 treatment of JUNV-infected cells at both 5 and 11 h p.i., in combination with a significant increase in the total number of autophagic structures and a ratio similar to that under EBSS conditions observed with the tandem protein (Fig. 1A and B and 2),
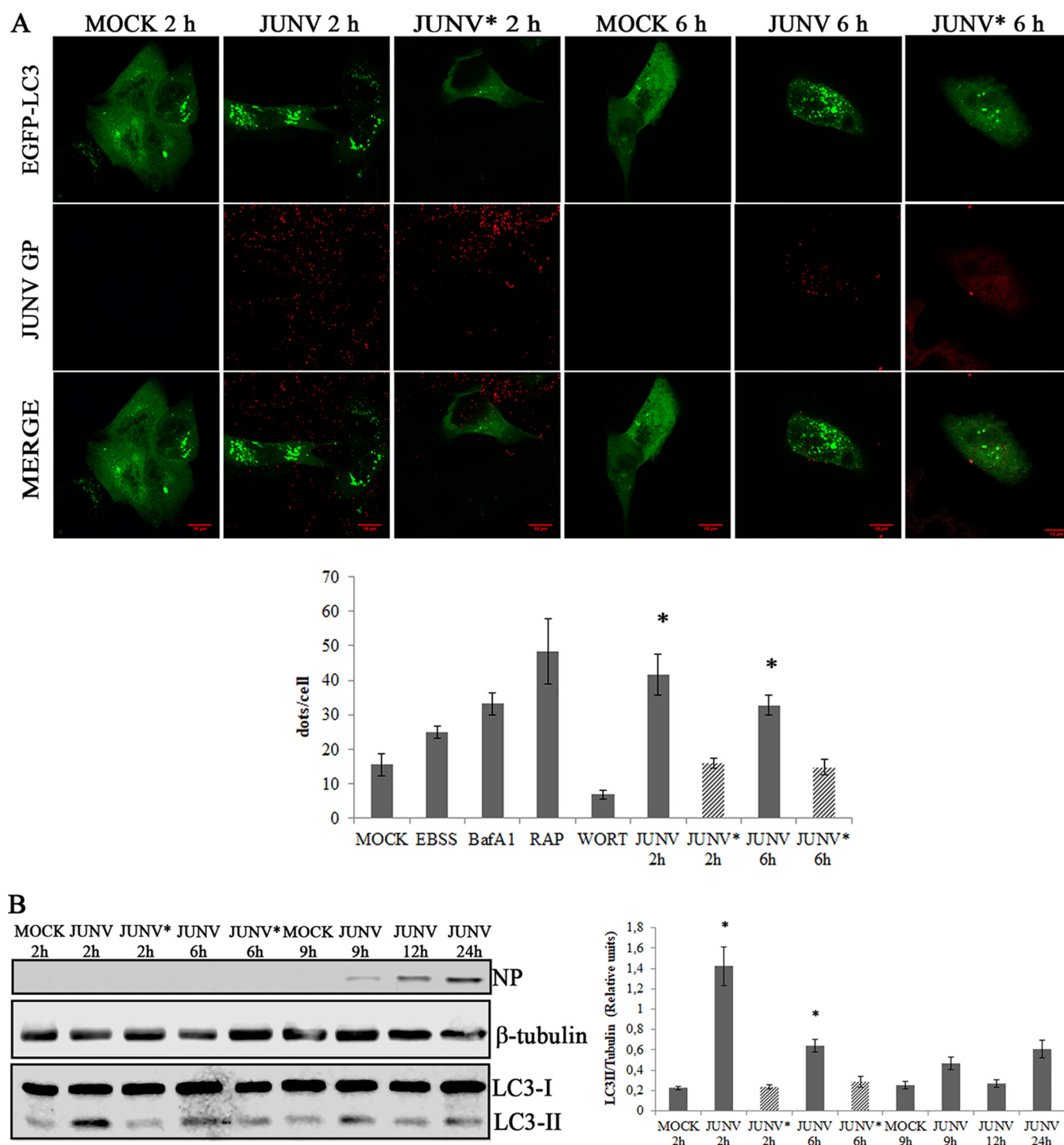
FIG 5 UV-inactivated JUNV infection does not induce LC3-II lipidation. A549 cells were transfected with a plasmid construct encoding EGFP-LC3. (A) Twenty-four hours posttransfection, cells were mock treated or treated with EBSS, 100 nM BafA1, 100 nM RAP, or 100 nM WORT or infected with JUNV or UV-inactivated JUNV (JUNV*) at an MOI of 1. After 2 h of treatment and at 2 or 6 h p.i., the cells were fixed and processed for immunofluorescence assay. An antibody against the JUNV GP was used, and the number of punctate structures was determined. Representative images were taken using a confocal microscope (Olympus FV 1000) (*, $P < 0.05$). (B) Twenty-four hours posttransfection, cells were mock treated or infected with JUNV or JUNV* at an MOI of 1. After 2 h of treatment and at different times p.i., the cells were processed for Western blotting using antibodies to EGFP, NP, and β-tubulin, followed by the corresponding peroxidase-conjugated secondary antibodies. The quantifications of the Western blot analysis were conducted as described in Materials and Methods (*, $P < 0.05$). The data represent means and SE. In all cases, a representative experiment from three independent experiments is shown.

demonstrated that the virus induces the autophagy pathway from 2 h p.i. without a substantial effect on autophagic flux.

To elucidate the role of JUNV-induced autophagy promotion in the viral life cycle, we observed that the infective ability was increased in cells with an augmented level of autophagy (Fig. 1C and D). Furthermore, the critical autophagy proteins Atg5 and Beclin 1 were required for the success of viral infection establishment, strongly pointing to a proviral role of the canonical pathway (Fig. 3 and 4). Moreover, the UV-inactivated virus was not able to induce the pathway, supporting the notion that active induction of autophagy is carried out by the virus for the benefit of its replication cycle (Fig. 5).

As obligatory intracellular parasites, virus survival is intimately associated with their ability not only to circumvent cellular processes that prevent their growth, but also to exploit host cell functions, such as autophagy, for their replication. Consequently, viruses have developed diversified strategies to avoid autophagy-mediated immune responses, allowing them to manipulate and exploit the autophagy pathway to their advantage. To date, the autophagic pathway and/or components of the autophagy machinery have been implicated in proviral roles for several RNA and DNA viruses (reviewed in reference 47). However, the precise molecular mechanisms of most proviral activities are scarcely known in the vast majority of cases. Notably, two critical questions arise from our observations: (i) what is the mechanism mediating autophagy induction by JUNV infection and (ii) what exactly is the role of autophagy in the virus replication cycle? Regarding the former, it was feasible to think about the autophagy induction as a consequence of virus-induced endoplasmic reticulum stress followed by an unfolded-protein response (ER-UPR). Indeed, growing evidence indicates that autophagy is induced by ER stress in organisms from *Saccharomyces cerevisiae* to mammals, and viral polypeptides synthesized during infection can stimulate ER stress (48). In turn, ER-induced autophagy may act as a protective mechanism to back up the ER-associated degradation pathway to help handle the cell burden under ER stress (49), or it can initiate programmed cell death if ER stress cannot be relieved (50). However, for JUNV, it has been reported that due to activation of the pattern recognition receptor protein kinase R (PKR) and upregulation of eIF2α phosphorylation, potent translational inhibition occurs during infection by the pathogenic Romero strain of JUNV in A549 cells at 48 h p.i. (51). Moreover, the authors demonstrated that a recombinant version of JUNV (rJUNV) expressing the Candid no. 1 strain-derived GPC protein caused ER stress due to levels of RNA synthesis and protein production higher than those in infection with rJUNV expressing the GPC protein of the pathogenic Romero strain of JUNV. They additionally showed that the impaired processing and altered trafficking of Candid no. 1 GPC were the causes of ER stress promotion and final apoptosis (52). We sought to study this possibility, which included the induction of autophagy as a consequence of the possible UPR-ER stress pathway triggered by our experimental conditions. Thus, A549 cells were infected with JUNV at an MOI of 1, and at 2, 6, and 12 h p.i., the monolayers were analyzed by Western blotting to detect intracellular levels of calnexin (CNX), an ER chaperone. Upon ER stress, upregulation of ER chaperones is pivotal for cell survival because it facilitates the correct folding and assembly of ER proteins and prevents their aggregation (53). Therefore, we analyzed the intracellular CNX level as a marker of UPR-ER in infected cells. As a positive control, we employed a 2-h treatment of A549 cells with tunicamycin (TM), a well-known ER stress inducer. While an apparent accumulation of CNX occurred after TM treatment, we did not observe a significant accumulation of CNX in JUNV-infected A549 cells at 2, 6, and 12 h p.i., suggesting the absence of a UPR-ER response after JUNV infection (data not shown).

On the other hand, regarding the induction mechanism, we nowadays count observations (58–60) in the JUNV field that allow us to answer this aspect, at least hypothetically. Cuevas and Ross demonstrated that murine macrophages, the initial targets of JUNV infection, sense JUNV through Toll-like receptor 2 (TLR-2)/TLR-6 heterodimers on the cell surface, leading to innate immune response activation characterized by the increased transcription levels of interferon beta and tumor necrosis factor

alpha (54). Since TLR signaling has been suggested to activate the autophagic pathway as well (55), we linked these two observations to hypothesize that TLR sensing might be responsible for autophagy induction by JUNV in the human A549 cell line. In this regard, it is vital to take into account that the innate immune response activation mediated by TLR-2 is independent of virus replication, as shown by Cuevas and collaborators (56). Therefore, even if it is possible that TLR-2 mediates autophagy induction, additional mechanisms, dependent on viral replication initiation, must be involved, since the inactivated virus was unable to trigger the pathway. Moreover, regarding the role of autophagy in JUNV replication, there are several possible ways in which autophagy might benefit viral infection. We focused on that derived from the fact that the autophagy pathway mediates dynamic membrane rearrangements inside the cell, which may facilitate the biogenesis of an intracellular membranous niche required for viral replication. In line with this possibility, Baird and collaborators, employing the nonpathogenic Tacaribe virus or the attenuated Candid no. 1 strain of JUNV, showed the cytosolic structures in which arenavirus replication and transcription take place. The authors analyzed the biochemical composition of the replication-transcription complexes (RTCs) induced by the virus and showed that several different cellular structures are involved. They observed a low buoyant density of RTCs, which, together with their sensitivity to nonionic detergents and their association with phosphatidylinositol 4 phosphate, strongly suggest that cellular membranes are mobilized for RTC formation (57). Thus, it seems likely that the autophagy machinery may collaborate in this crucial step of the arenavirus replication process, an aspect that we are planning to explore in our laboratory.

In conclusion, in this study, we found that the early activation of the autophagy pathway upon JUNV infection of A549 human cells has a proviral role, supporting efficient viral infection establishment. Our understanding of the molecular mechanisms underlying the interplay between JUNV and autophagy is still insufficient, and further investigations are necessary to comprehend the exact molecular mechanism by which the virus induces the pathway and how the autophagy machinery supports JUNV infection in these cells. Nevertheless, we consider our present data especially relevant, since they comprise the first evidence for the elucidation of the role of autophagy in the field of arenavirus replication. Indeed, these observations constitute the keystone of the field, aiding in the direction of the discovery of new molecular targets to design therapeutic approaches to arenavirus infection.

MATERIALS AND METHODS

Cell lines, virus, and plasmids. Human lung epithelial A549 cells (ATCC no. CCL-185) were grown in MEM (Life Technologies, Argentina) containing 10% heat-inactivated FCS (Life Technologies, Argentina) and supplemented with 50 μg/ml gentamicin and incubated at 37°C in an atmosphere of 5% CO_2. $atg5^{-/-}$ and WT MEFs (provided by Noboru Mizushima, University of Tokyo, Tokyo, Japan) were maintained in Dulbecco's modified Eagle medium (DMEM) (Life Technologies, Argentina) containing 10% heat-inactivated FCS and supplemented with 50 μg/ml gentamicin and incubated at 37°C in an atmosphere of 5% CO_2. The naturally attenuated Junín virus strain IV$_{4454}$ (58), employed in all the experiments, was propagated in Vero cells (ATCC no. CCL-81). Virus yield was determined by PFU assay in Vero cells as described previously (59). JUNV was inactivated by UV irradiation as described previously (60). Inactivation was verified by PFU assay in the above-mentioned cells. A plasmid encoding EGFP-microtubule-associated protein light chain 3 (pEGFP-LC3) was kindly provided by Noboru Mizushima (Tokyo Medical and Dental University). pBeclin 1-KD (a pSuper.retro.puro vector in which the oligonucleotide sequence used for siRNA interference with Beclin 1 expression has been inserted) and the empty plasmid were provided by William S. Maltese (Medical University of Ohio, Toledo, OH, USA). A tandem fusion protein of mCherry and GFP fused to LC3B (one of the members of the mammalian LC3 family) to make a pH-sensitive sensor that is used to monitor autophagy in live cells, mCherry-GFP-LC3, was kindly provided by D. Terje Johansen (30). A plasmid construction encoding the Atg5 protein was kindly provided by Tamotsu Yoshimori (Osaka, Japan) and employed for $atg5^{-/-}$ MEF complementation.

Reagent and antibodies. BafA1, WORT, RAP, a polyclonal antibody against LC3, and monoclonal antibodies against β-tubulin were purchased from Sigma-Aldrich (Argentina) and prepared following the manufacturer's instructions. For some experiments, cells were incubated in starvation medium, EBSS, purchased from Life Technologies (Argentina). Alexa 488–goat anti-rabbit, Alexa 568–goat anti-rabbit, Alexa 488–goat anti-mouse, Alexa 568–goat anti-mouse, and Alexa 647–goat anti-mouse secondary antibodies were also purchased from Life Technologies (Argentina). Monoclonal antibodies against JUNV

NP and virus GP were kindly provided by A. Sanchez (CDC, Atlanta, GA, USA) (61). Whole rabbit antiserum against EGFP was kindly provided by Martín Monte (FCEN, IQUIBICEN, UBA, Argentina).

Transient transfections and infections. A549 cells were grown on coverslips to 50% confluence in 24-well plates and transfected with Lipofectamine 2000 (Life Technologies, Argentina) according to the manufacturer's recommendations. After 24 h of transfection, the cells were subjected to different treatments and analyzed by epifluorescence microscopy or Western blotting. For $atg5^{-/-}$ complementation experiments, MEFs were grown on coverslips to 50% confluence in a 24-well plate and transfected with polyethylenimine, branched (PEI) (Sigma-Aldrich, Argentina), according to the manufacturer's recommendations. Viral infections were carried out with Junín IV$_{4454}$ virions at an MOI of 1 PFU/cell. After 60 min of virus adsorption, the cells were washed, fresh medium was added, and the infection was allowed to proceed at 37°C for 2 to 48 h, depending on the assay. When indicated, EBSS, WORT, or RAP was added before the infected and mock-infected cells.

Fluorescence microscopy. (i) Direct immunofluorescence. pEGFP-LC3- or pmCherry-GFP-LC3-transfected A549 cells were infected or not (mock infected) with JUNV for 2, 6, 9, 12, and 24 h. When assaying the UV-inactivated virus, we tested only 2 and 6 h of infection. Then, the cells were washed three times with phosphate-buffered saline (PBS), fixed with freshly prepared 4% formaldehyde solution in PBS for 15 min at room temperature, permeabilized with 0.2% Triton X-100, and incubated with the corresponding antibodies to detect the infected cells. Subsequently, the cells were washed three times with PBS, mounted with buffered glycerol, and analyzed by fluorescence microscopy using a confocal Olympus FV1000 microscope. For quantification of punctate structures, all the images were processed using ImageJ software (Wayne Rasband, National Institutes of Health). After image binarization using a defined threshold, the dots were quantified using the Particle Analyzer plugin.

(ii) Indirect immunofluorescence. A549 cells were treated with EBSS, WORT, BafA1, or RAP or left under control conditions for 2 h. After that period, the cells were infected with JUNV as described above. In the experiments employing WT and $atg5^{-/-}$ MEFs, to optimize the infection conditions, the cells were centrifuged for 30 min at 1.000 × g during JUNV inoculation (termed "spinoculation") without pretreatment. At 24 and 48 h p.i., the cells were washed three times with PBS, fixed as described for direct immunofluorescence, permeabilized with 0.2% Triton X-100, and incubated with the monoclonal antibody for the viral NP or with the monoclonal antibody for the viral GP for identification of infected cells or with polyclonal antibody against LC3 when using MEFs. Anti-NP bound antibodies were detected by incubation with Alexa 488-goat anti-mouse antibody, and anti-GP bound antibodies were detected by incubation with Alexa 647-goat anti-mouse antibody (tandem experiment) or Alexa 568-goat anti-mouse antibody (UV inactivated virus experiment). Anti-LC3 bound antibodies were detected by incubation with Alexa 568-goat anti-rabbit antibody. Nuclei were stained with Hoechst 33342. The cells were mounted with buffered glycerol and examined with an Olympus BX51 or confocal Olympus FV1000 microscope. The data in the figures represent the means and standard errors (SE) obtained after analyzing 100 cells per condition from at least three independent experiments. Representative images are shown for each case.

Western blotting. Protein samples of a total cell lysate from A549 cells or pEGFP-LC3-transfected A549 cells infected with JUNV and treated with EBSS, WORT, BafA1, RAP, or control were prepared. Infected WT and $atg5^{-/-}$ MEF lysates were also analyzed. Briefly, the cells were washed three times with PBS and lysed in dithiothreitol (DTT) buffer. Whole-cell lysates were separated in SDS-PAGE gels (15% for endogenous LC3 and 10% for EGFP-LC3 detection) and transferred to polyvinylidene difluoride (PVDF) membranes. The membranes were blocked with 3% skim milk in Tris-buffered saline (TBS) for 1 h at room temperature, followed by incubation with antibodies against LC3 or NP in PBS or β-tubulin or EGFP in 3% skim milk in TBS at 4°C overnight. The membranes were then incubated with the appropriate horseradish peroxidase-conjugated secondary antibodies in 3% skim milk in TBS at room temperature for 2 h, followed by detection with an enhanced-chemiluminescence detection kit from GE Healthcare (Amersham, UK; RPN2109). The protein band intensities from three independent experiments were quantitated with FIJI software (62) and normalized against β-tubulin. Representative images are shown for each case.

Statistical analysis. Two-tailed analysis of variance (ANOVA) with Tukey's test was used to determine statistical significance in fluorescence and Western blot experiments. In all graphs, the results are shown as the means and SE of the results of at least three independent experiments normalized to the control treatment. A P value of 0.05 was considered statistically significant. The InfoStat program (63) was used to conduct the analyses.

REFERENCES

1. Buchmeier MJ. 2007. Arenaviridae: the virus and their replication, p 1792–1827. In Knipe DM, Howley PM, Griffin DE, Lamb RA, Martin MA, Roizman B, Straus SE (ed), Fields Virology, 5th ed, vol 2. Lippincott Williams & Wilkins, Philadelphia, PA.

2. Charrel RN, de Lamballerie X, Emonet S. 2008. Phylogeny of the genus Arenavirus. Curr Opin Microbiol 11:362–368. https://doi.org/10.1016/j.mib.2008.06.001.

3. Briese T, Paweska JT, McMullan LK, Hutchison SK, Street C, Palacios G, Khristova ML, Weyer J, Swanepoel R, Egholm M, Nichol ST, Lipkin WI. 2009. Genetic detection and characterization of Lujo virus, a new hemorrhagic fever–associated arenavirus from Southern Africa. PLoS Pathog 5:e1000455. https://doi.org/10.1371/journal.ppat.1000455.

4. Frame JD, Gocke DJ, Baldwin JM, Troup JM. 1970. Lassa fever, a new virus disease of man from West Africa. Am J Trop Med Hyg 19:670–676. https://doi.org/10.4269/ajtmh.1970.19.670.

5. Parodi AS, Greenway DJ, Rugiero HR, Frigerio M, De La Barrera JM, Mettler N, Garzon F, Boxaca M, Guerrero L, Nota N. 1958. Concerning the epidemic outbreak in Junin. Dia Med 30:2300–2301.

6. Maiztegui JI, McKee KT, Jr, Oro JGB, Harrison LH, Gibbs PH, Feuillade MR, Enria DA, Briggiler AM, Levis SC, Ambrosio AM, Halsey NA, Peters CJ. 1998. Protective efficacy of a live attenuated vaccine against Argentine hemorrhagic fever. J Infect Dis 177:277–283. https://doi.org/10.1086/514211.

7. Harnish DG, Dimock K, Bishop DH, Rawls WE. 1983. Gene mapping in Pichinde virus: assignment of viral polypeptides to genomic L and S RNAs. J Virol 46:638–641.

8. York J, Romanowski V, Lu M, Nunberg JH. 2004. The signal peptide of the Junín arenavirus envelope glycoprotein is myristoylated and forms an essential subunit of the mature G1-G2 complex. J Virol 78:10783–10792. https://doi.org/10.1128/JVI.78.19.10783-10792.2004.

9. Cao W, Henry MD, Borrow P, Yamada H, Elder JH, Ravkov EV, Nichol ST, Compans RW, Campbell KP, Oldstone MB. 1998. Identification of alpha-dystroglycan as a receptor for lymphocytic choriomeningitis virus and Lassa fever virus. Science 282:2079–2081. https://doi.org/10.1126/science.282.5396.2079.

10. Spiropoulou CF, Kunz S, Rollin PE, Campbell KP, Oldstone M. 2002. New World arenavirus clade C, but not clade A and B viruses, utilizes alpha-dystroglycan as its major receptor. J Virol 76:5140–5146. https://doi.org/10.1128/JVI.76.10.5140-5146.2002.

11. Radoshitzky SR, Abraham J, Spiropoulou CF, Kuhn JH, Nguyen D, Li W, Nagel J, Schmidt PJ, Nunberg JH, Andrews NC, Farzan M, Choe H. 2007. Transferrin receptor 1 is a cellular receptor for New World haemorrhagic fever arenaviruses. Nature 446:92–96. https://doi.org/10.1038/nature05539.

12. Martinez MG, Bialecki MA, Belouzard S, Cordo SM, Candurra NA, Whittaker GR. 2013. Utilization of human DC-SIGN and L-SIGN for entry and infection of host cells by the New World arenavirus, Junín virus. Biochem Biophys Res Commun 441:612–617. https://doi.org/10.1016/j.bbrc.2013.10.106.

13. Castilla V, Mersich SE, Candurra NA, Damonte EB. 1994. The entry of Junin virus into Vero cells. Arch Virol 136:363–374. https://doi.org/10.1007/BF01321064.

14. Yang Z, Klionsky DJ. 2010. Eaten alive: a history of macroautophagy. Nat Cell Biol 12:814. https://doi.org/10.1038/ncb0910-814.

15. Shoji-Kawata S, Levine B. 2009. Autophagy, antiviral immunity, and viral countermeasures. Biochim Biophys Acta 1793:1478–1484. https://doi.org/10.1016/j.bbamcr.2009.02.008.

16. Amaya C, Fader CM, Colombo MI. 2015. Autophagy and proteins involved in vesicular trafficking. FEBS Lett 589:3343–3353. https://doi.org/10.1016/j.febslet.2015.09.021.

17. Jackson WT. 2015. Viruses and the autophagy pathway. Virology 479-480:450–456. https://doi.org/10.1016/j.virol.2015.03.042.

18. Ke P-Y, Chen SS. 2011. Autophagy: a novel guardian of HCV against innate immune response. Autophagy 7:533–535. https://doi.org/10.4161/auto.7.5.14732.

19. Lee Y-R, Lei H-Y, Liu M-T, Wang J-R, Chen S-H, Jiang-Shieh Y-F, Lin Y-S, Yeh T-M, Liu C-C, Liu H-S. 2008. Autophagic machinery activated by dengue virus enhances virus replication. Virology 374:240–248. https://doi.org/10.1016/j.virol.2008.02.016.

20. Taylor MP, Kirkegaard K. 2007. Modification of cellular autophagy protein LC3 by poliovirus. J Virol 81:12543–12553. https://doi.org/10.1128/JVI.00755-07.

21. Chaumorcel M, Souquère S, Pierron G, Codogno P, Esclatine A. 2008. Human cytomegalovirus controls a new autophagy-dependent cellular antiviral defense mechanism. Autophagy 4:46–53. https://doi.org/10.4161/auto.5184.

22. Leidal AM, Cyr DP, Hill RJ, Lee PWK, McCormick C. 2012. Subversion of autophagy by Kaposi's sarcoma-associated herpesvirus impairs oncogene-induced senescence. Cell Host Microbe 11:167–180. https://doi.org/10.1016/j.chom.2012.01.005.

23. Tallóczy Z, Virgin H IV, Levine B. 2006. PKR-dependent xenophagic degradation of herpes simplex virus type 1. Autophagy 2:24–29. https://doi.org/10.4161/auto.2176.

24. Chiramel A, Brady N, Bartenschlager R. 2013. Divergent roles of autophagy in virus infection. Cells 2:83–104. https://doi.org/10.3390/cells2010083.

25. Kabeya Y, Mizushima N, Ueno T, Yamamoto A, Kirisako T, Noda T, Kominami E, Ohsumi Y, Yoshimori T. 2000. LC3, a mammalian homologue of yeast Apg8p, is localized in autophagosome membranes after processing. EMBO J 19:5720–5728. https://doi.org/10.1093/emboj/19.21.5720.

26. Noda T, Ohsumi Y. 1998. Tor, a phosphatidylinositol kinase homologue, controls autophagy in yeast. J Biol Chem 273:3963–3966. https://doi.org/10.1074/jbc.273.7.3963.

27. Blommaart EFC, Krause U, Schellens JPM, Vreeling-Sindelarova H, Meijer AJ. 1997. The phosphatidylinositol 3-kinase inhibitors wortmannin and LY294002 inhibit autophagy in isolated rat hepatocytes. Eur J Biochem 243:240–246. https://doi.org/10.1111/j.1432-1033.1997.0240a.x.

28. Mizushima N, Yoshimori T. 2007. How to interpret LC3 immunoblotting. Autophagy 3:542–545. https://doi.org/10.4161/auto.4600.

29. Mizushima N, Yoshimori T, Levine B. 2010. Methods in mammalian autophagy research. Cell 140:313–326. https://doi.org/10.1016/j.cell.2010.01.028.

30. Hansen TE, Johansen T. 2011. Following autophagy step by step. BMC Biol 9:39. https://doi.org/10.1186/1741-7007-9-39.

31. Mizushima N, Yamamoto A, Hatano M, Kobayashi Y, Kabeya Y, Suzuki K, Tokuhisa T, Ohsumi Y, Yoshimori T. 2001. Dissection of autophagosome formation using Apg5-deficient mouse embryonic stem cells. J Cell Biol 152:657–668. https://doi.org/10.1083/jcb.152.4.657.

32. Berryman S, Brooks E, Burman A, Hawes P, Roberts R, Netherton C, Monaghan P, Whelband M, Cottam E, Elazar Z, Jackson T, Wileman T. 2012. Foot-and-mouth disease virus induces autophagosomes during cell entry via a class III phosphatidylinositol 3-kinase-independent pathway. J Virol 86:12940–12953. https://doi.org/10.1128/JVI.00846-12.

33. Gannagé M, Dormann D, Albrecht R, Dengjel J, Torossi T, Rämer PC, Lee M, Strowig T, Arrey F, Conenello G, Pypaert M, Andersen J, García-Sastre A, Münz C. 2009. Matrix protein 2 of influenza A virus blocks autophagosome fusion with lysosomes. Cell Host Microbe 6:367–380. https://doi.org/10.1016/j.chom.2009.09.005.

34. Kobayashi S, Orba Y, Yamaguchi H, Takahashi K, Sasaki M, Hasebe R, Kimura T, Sawa H. 2014. Autophagy inhibits viral genome replication and gene expression stages in West Nile virus infection. Virus Res 191:83–91. https://doi.org/10.1016/j.virusres.2014.07.016.

35. Funderburk SF, Wang QJ, Yue Z. 2010. The Beclin 1–VPS34 complex—at the crossroads of autophagy and beyond. Trends Cell Biol 20:355–362. https://doi.org/10.1016/j.tcb.2010.03.002.

36. Matsunaga K, Saitoh T, Tabata K, Omori H, Satoh T, Kurotori N, Maejima I, Shirahama-Noda K, Ichimura T, Isobe T, Akira S, Noda T, Yoshimori T. 2009. Two Beclin 1-binding proteins, Atg14L and Rubicon, reciprocally regulate autophagy at different stages. Nat Cell Biol 11:385–396. https://doi.org/10.1038/ncb1846.

37. Scarlatti F, Maffei R, Beau I, Ghidoni R, Codogno P. 2008. Non-canonical autophagy: an exception or an underestimated form of autophagy? Autophagy 4:1083–1085. https://doi.org/10.4161/auto.7068.

38. Gao P, Bauvy C, Souquère S, Tonelli G, Liu L, Zhu Y, Qiao Z, Bakula D, Proikas-Cezanne T, Pierron G, Codogno P, Chen Q, Mehrpour M. 2010. The Bcl-2 homology domain 3 mimetic gossypol induces both Beclin 1-dependent and Beclin 1-independent cytoprotective autophagy in cancer cells. J Biol Chem 285:25570–25581. https://doi.org/10.1074/jbc.M110.118125.

39. Mauthe M, Jacob A, Freiberger S, Hentschel K, Stierhof Y-D, Codogno

P, Proikas-Cezanne T. 2011. Resveratrol-mediated autophagy requires WIPI-1-regulated LC3 lipidation in the absence of induced phago-phore formation. Autophagy 7:1448–1461. https://doi.org/10.4161/auto.7.12.17802.

40. Scarlatti F, Maffei R, Beau I, Codogno P, Ghidoni R. 2008. Role of non-canonical Beclin 1-independent autophagy in cell death induced by resveratrol in human breast cancer cells. Cell Death Differ 15:1318–1329. https://doi.org/10.1038/cdd.2008.51.

41. Smith DM, Patel S, Raffoul F, Haller E, Mills GB, Nanjundan M. 2010. Arsenic trioxide induces a beclin-1-independent autophagic pathway via modulation of SnoN/SkiL expression in ovarian carcinoma cells. Cell Death Differ 17:1867–1881. https://doi.org/10.1038/cdd.2010.53.

42. Wong CH, Iskandar KB, Yadav SK, Hirpara JL, Loh T, Pervaiz S. 2010. Simultaneous induction of non-canonical autophagy and apoptosis in cancer cells by ROS-dependent ERK and JNK activation. PLoS One 5:e9996. https://doi.org/10.1371/journal.pone.0009996.

43. Mestre MB, Colombo MI. 2012. cAMP and EPAC are key players in the regulation of the signal transduction pathway involved in the α-hemolysin autophagic response. PLoS Pathog 8:e1002664. https://doi.org/10.1371/journal.ppat.1002664.

44. Flanagan ML, Oldenburg J, Reignier T, Holt N, Hamilton GA, Martin VK, Cannon PM. 2008. New World clade b arenaviruses can use transferrin receptor 1 (TfR1)-dependent and -independent entry pathways, and glycoproteins from human pathogenic strains are associated with the use of TfR1. J Virol 82:938–948. https://doi.org/10.1128/JVI.01397-07.

45. Di Simone C, Buchmeier MJ. 1995. Kinetics and pH dependence of acid-induced structural changes in the lymphocytic choriomeningitis virus glycoprotein complex. Virology 209:3–9. https://doi.org/10.1006/viro.1995.1225.

46. Di Simone C, Zandonatti MA, Buchmeier MJ. 1994. Acidic pH triggers LCMV membrane fusion activity and conformational change in the glycoprotein spike. Virology 198:455–465. https://doi.org/10.1006/viro.1994.1057.

47. Dong X, Levine B. 2013. Autophagy and viruses: adversaries or allies? J Innate Immun 5:480–493. https://doi.org/10.1159/000346388.

48. He B. 2006. Viruses, endoplasmic reticulum stress, and interferon re-sponses. Cell Death Differ 13:393–403. https://doi.org/10.1038/sj.cdd.4401833.

49. Yorimitsu T, Nair U, Yang Z, Klionsky DJ. 2006. Endoplasmic reticulum stress triggers autophagy. J Biol Chem 281:30299–30304. https://doi.org/10.1074/jbc.M607007200.

50. Maiuri MC, Zalckvar E, Kimchi A, Kroemer G. 2007. Self-eating and self-killing: crosstalk between autophagy and apoptosis. Nat Rev Mol Cell Biol 8:741–752. https://doi.org/10.1038/nrm2239.

51. Huang C, Kolokoltsova OA, Mateer EJ, Koma T, Paessler S. 2017. Highly pathogenic New World arenavirus infection activates the pattern recog-nition receptor protein kinase R without attenuating virus replication in human cells. J Virol 91:e01090-17. https://doi.org/10.1128/JVI.01090-1.

52. Manning JT, Seregin AV, Yun NE, Koma T, Huang C, Barral J, de la Torre JC, Paessler S. 2017. Absence of an N-linked glycosylation motif in the glycoprotein of the live-attenuated Argentine hemorrhagic fever vac-cine, Candid #1, results in its improper processing, and reduced surface expression. Front Cell Infect Microbiol 7:20. https://doi.org/10.3389/fcimb.2017.00020.

53. Schröder M. 2008. Endoplasmic reticulum stress responses. Cell Mol Life Sci 65:862–894. https://doi.org/10.1007/s00018-007-7383-5.

54. Cuevas CD, Ross SR. 2014. Toll-like receptor 2-mediated innate immune responses against Junín virus in mice lead to antiviral adaptive immune responses during systemic infection and do not affect viral replication in the brain. J Virol 88:7703–7714. https://doi.org/10.1128/JVI.00050-14.

55. Delgado MA, Elmaoued RA, Davis AS, Kyei G, Deretic V. 2008. Toll-like receptors control autophagy. EMBO J 27:1110–1121. https://doi.org/10.1038/emboj.2008.31.

56. Cuevas CD, Lavanya M, Wang E, Ross SR. 2011. Junin virus infects mouse cells and induces innate immune responses. J Virol 85:11058–11068. https://doi.org/10.1128/JVI.05304-11.

57. Baird NL, York J, Nunberg JH. 2012. Arenavirus infection induces discrete cytosolic structures for RNA replication. J Virol 86:11301–11310. https://doi.org/10.1128/JVI.01635-12.

58. Weissenbacher MC, Sabattini MS, Avila MM, Sangiorgio PM, de Sensi MR, Contigiani MS, Levis SC, Maiztegui JI. 1983. Junin virus activity in two rural populations of the Argentine hemorrhagic fever (AHF) endemic area. J Med Virol 12:273–280. https://doi.org/10.1002/jmv.1890120407.

59. Groseth A, Hoenen T, Weber M, Wolff S, Herwig A, Kaufmann A, Becker S. 2011. Tacaribe virus but not Junin virus infection induces cytokine release from primary human monocytes and macrophages. PLoS Negl Trop Dis 5:e1137. https://doi.org/10.1371/journal.pntd.0001137.

60. Linero FN, Scolaro LA. 2009. Participation of the phosphatidylinositol 3-kinase/Akt pathway in Junín virus replication in vitro. Virus Res 145:166–170. https://doi.org/10.1016/j.virusres.2009.07.004.

61. Sanchez A, Pifat DY, Kenyon RH, Peters CJ, McCormick JB, Kiley MP. 1989. Junin virus monoclonal antibodies: characterization and cross-reactivity with other arenaviruses. J Gen Virol 70:1125–1132. https://doi.org/10.1099/0022-1317-70-5-1125.

62. Schindelin J, Arganda-Carreras I, Frise E, Kaynig V, Longair M, Pietzsch T, Pietzsch T, Preibisch S, Rueden C, Saalfeld S, Schmid B, Tinevez JY, White DJ, Hartenstein V, Eliceiri K, Tomancak P, Cardona A. 2012. Fiji: an open-source platform for biological-image analysis. Nat Methods 9:676–682. https://doi.org/10.1038/nmeth.2019.

63. Di Rienzo JA, Casanoves F, Balzarini M, Gonzalez L, Tablada M, Robledo CW. 2014. InfoStat statistical software. National University of Córdoba, Córdoba, Argentina.